Virology **300,** 140–152 (2002)
doi:10.1006/viro.2002.1550

Mutational Analysis of the Replication Signals in the 3′-Nontranslated Region of *Citrus Tristeza Virus*

Tatineni Satyanarayana, Siddarame Gowda, María A. Ayllón, María R. Albiach-Martí, and William O. Dawson[1]

Citrus Research and Education Center, University of Florida, Lake Alfred, Florida 33850

Received March 5, 2002; returned to author April 15, 2002; accepted May 7, 2002

Citrus tristeza virus (CTV), a member of the *Closteroviridae,* has a 19.3-kb messenger-sense RNA genome consisting of 12 open reading frames with nontranslated regions (NTR) at the 5′ and 3′ termini. The 273 nucleotide (nt) 3′-NTR is highly conserved (~95%) among the sequenced CTV isolates in contrast to the highly diverse 5′-NTR sequences. The 3′ replication signals were mapped to the 3′ 234 nts within the NTR. This region of CTV does not contain a poly-A tract nor does it appear to fold as a tRNA-mimic. Instead, a computer-predicted thermodynamically stable secondary structure comprised of 10 stem-and-loop (SL) structures, referred to as SL1 to SL10 (5′ to 3′), was common to all CTV isolates. This putative structure was used as a guide to examine the 3′ requirements for replication *in vivo.* The resulting data suggest that a complex 3′ structure is required for those functions that provide for efficient replication of CTV *in vivo* such as minus-strand initiation, regulation of strand asymmetry, effective translation of the myriad of viral mRNAs, or stability of RNAs. Deletions into the 3′-NTR, up to 66 nts from the 5′ direction and 11 nts from the 3′ direction, deleting or disrupting putative SL1, SL2 and SL3, or SL10, resulted in continued replication, suggesting that these sequences are not essential for basal-level replication, but are required for efficient replication. Predicted stem loops 3 through 10 were examined by mutations designed to alter the primary structures while preserving the secondary structures. Mutations designed to disrupt the predicted stems of SL3, SL5, SL7, SL9, or SL10 resulted in substantially reduced levels of replication, while compensatory mutations resulted in partial restorations of replication, suggesting that these predicted secondary structures are involved in replication. Also, the putative loop sequences of SL5, SL6, SL7, and SL9 tolerated mutagenesis with continued but reduced levels of replication. In contrast, all mutations introduced into putative SL4, SL8, and the stem of SL6 prevented replication, suggesting that the primary structure of these regions make up the core of the 3′ replication signal. The 3′ triplet, CCA, was shown to be necessary for efficient replication, but deletion of eleven nts to expose an internal CCA resulted in continued replication.

INTRODUCTION

Positive-stranded RNA viruses generally have replication signals, which are primary or higher-ordered structures usually residing near the 5′ and 3′ termini, that are required for replication of that RNA (Buck, 1996; Chapman and Kao, 1999; Sivakumaran *et al.,* 1999). The 3′-terminal *cis*-acting elements tend to be more conserved and complex than the 5′-*cis*-acting elements (Dreher, 1999). The 3′ termini usually are composed of tRNA-like structures, poly (A) tails, or relatively undefined structures that often can be folded into stem-and-loop (SL) structures. Although the three types of 3′-terminal structures are not exclusively clustered in phylogenies based on the sequence similarities of viral RNA-dependent RNA polymerase (RdRp), they are conserved among the different RNAs of multipartite viruses and within virus groups (Koonin and Dolja, 1993; Dreher, 1999).

An integral function of the 3′ *cis*-acting elements which has been extensively examined is the initiation of complementary negative strands (Duggal *et al.,* 1994; Lai, 1998; Dreher, 1999). When minus-strand promotion has been examined *in vitro* with purified replicase preparations, in the simplest cases, only a CC(A/G) "initiation box" is sufficient to begin minus-strand synthesis (Yoshinari *et al.,* 2000). Yet, comparison of a range of replicases demonstrates that higher-order structures are also important for either presentation of the CC(A/G) motif or as a promoter element for replicase binding (Song and Simon, 1995; Kim *et al.,* 2000; Osman *et al.,* 2000). Thus, among different positive-stranded RNA viruses, there appears to be a continuum from simply needing an available initiation box to controlling by complex structural elements. However, the 3′ signals required for *in vivo* replication generally are much more extensive than what are required for *in vitro* minus-strand initiation (Carpenter and Simon, 1998; Dreher, 1999; Chandrika *et al.,* 2000; Osman *et al.,* 2000). Why the requirement for a more complex replication signal *in vivo?* 3′-Terminal regions also have been shown to be required for other functions: as telomeres to retain 3′ nucleotides; as modulators of

[1] To whom correspondence and reprint requests should be addressed at Citrus Research and Education Center, University of Florida, 700 Experiment Station Road, Lake Alfred, FL 33850. Fax: (863) 956-4631. E-mail: wodtmv@lal.ufl.edu.

0042-6822/02 $35.00

translation; and sometimes they can be involved in RNA stability, cellular targeting, and packaging (Dreher, 1999). Additionally, a new function recently proposed is inhibition of minus-strand synthesis (Singh and Dreher, 1998; Dreher, 1999; Koev *et al.,* 2002). In general, positive-stranded RNA viruses produce negative strands as template early during infection and later produce primarily positive-stranded RNAs. It is possible that 3′ structures function to prevent initiation of negative strands late in the infection. Thus, the viral 3′ *cis*-acting elements serve multiple functions during replication.

Citrus tristeza virus (CTV) is a member of the *Closterovirus* genus of the *Closteroviridae,* a family that contains viruses with mono- and bi-partite genomes transmitted by different insect vectors including aphids, whiteflies, and mealybugs (Dolja *et al.,* 1994; Karasev, 2000). The 19.3-kb single-stranded, positive-sense RNA genome of CTV consists of 12 open reading frames (ORFs) (Pappu *et al.,* 1994; Karasev *et al.,* 1995). The 5′-proximal ORF 1a encodes a 349-kDa polyprotein containing two papain protease-like domains plus methyltransferase-like and helicase-like domains. ORF 1b encodes an RdRp-like domain thought to be translated by a +1 frameshift from ORF 1a to produce an ~400-kDa polyprotein (Karasev *et al.,* 1995). Ten 3′ ORFs are expressed by 3′-coterminal subgenomic RNAs (sgRNAs) that are promoted and/or terminated internally at controller elements (Hilf *et al.,* 1995; Gowda *et al.,* 2001). The polar helical virions are encapsidated primarily with the major coat protein, but one end (approximately 5% of virion length) is encapsidated with the minor coat protein (Febres *et al.,* 1996). In addition to the two coat proteins, the HSP70-like protein (p65) plus the p61 protein are also involved in virion assembly (Satyanarayana *et al.,* 2000). Recently, the p20 and p23 proteins were found to be an inclusion body protein and a regulatory protein that controls asymmetrical RNA accumulation, respectively (Gowda *et al.,* 2000; Satyanarayana *et al.,* 2002). No functions have been associated with the other four 3′ ORFs.

The 5′-nontranslated region (NTR) consists of 107 nts, and the 3′-NTR consists of 273 nts. Among the different CTV isolates for which sequence is available, the 3′ terminal sequences are much more conserved than the 5′ terminal sequences; this is due to the unusual sequence variation among different CTV isolates. Although the sequence divergence among some isolates is relatively uniform throughout the genome, other isolates show asymmetrical homology that decreases from approximately 90% identity in the 3′ half of the genome to as little as 42% toward the 5′ terminus (Mawassi *et al.,* 1996; Albiach-Martí *et al.,* 2000). However, even though the 5′ termini differ substantially in sequence, the predicted secondary structures, two stem-and-loops, are maintained in different CTV isolates, suggesting that secondary structures rather than primary structures are important replication signals (López *et al.,* 1998; Gowda, unpublished data). In contrast, the known 3′ terminal sequences are almost identical. Yet, near-identical heterologous 3′ termini substantially decrease CTV RNA replication (Satyanarayana *et al.,* 1999). The 30–50% reduction of replication due to exchanges of 3′-NTR's from isolates VT or T30 into isolate T36 of CTV suggests only partial compatibility of T36 replicase complex with the heterologous 3′-*cis*-acting elements. What are the characteristics of the *cis*-acting elements in the 3′ terminal sequences of CTV that determines efficient replication?

Here we describe a complex 3′ structure required for CTV replication. The sequences of the 3′-NTRs of different CTV isolates were compared and their potential secondary structures were estimated using the *MFOLD* program as a series of 10 stem-and-loop (SL) structures. Mutations designed to alter primary structure while preserving secondary structure showed that the different SLs varied in ability to tolerate primary or secondary structure mutations.

RESULTS AND DISCUSSION

Rationale for analysis of 3′-*cis*-acting elements in CTV-ΔCla

We previously showed that the CTV replicon, CTV-ΔCla, which has the 3′ ORFs deleted, replicated efficiently in *Nicotiana benthamiana* mesophyll protoplasts (Satyanarayana *et al.,* 1999). Because of its smaller size and the gain of some unique restriction sites in the cDNA, this replicon provides a much easier genetic system than the full-length virus to examine the 3′-*cis*-acting elements. CTV-ΔCla contains the 5′-NTR plus ORFs 1a and 1b and the first 105 nts of ORF2 (nts 1–11011) fused to the 3′ 768 nts of the genomic RNA that includes part of the p23 ORF and the 3′-NTR (nts 18529–19296) (Fig. 1A; Satyanarayana *et al.,* 1999). Mutations can be created directly within pCTV-ΔCla with one step ligations between *Cla*I and *Not*I restriction endonuclease sites, compared to multiple ligation steps using the full-length virus. Additionally, the smaller replicon (~12.0 kb) resulted in more efficient transfection of protoplasts (Satyanarayana *et al.,* 2001). Analysis of protoplasts inoculated with CTV-ΔCla revealed the accumulation of positive- and negative-stranded RNAs of both the genomic RNA (11.8 kb) and the one hybrid p33/p23 sgRNA (~0.9 kb) due to the residual p33 controller element in a near-symmetrical fashion at ratios of ~1:1 to 2:1 (Satyanarayana *et al.,* 2002; Fig. 1B, a).

Defining a minimal 3′-*cis*-acting element

Previously, we demonstrated that 3′-replication signals of CTV were located within the 3′-NTR by deleting the remaining p23 sequence from CTV-ΔCla to obtain CTV-ΔCla-3′NTR without significant loss of replication (Satyanarayana *et al.,* 1999; see Fig. 1, CTV-ΔCla-3′NTR).

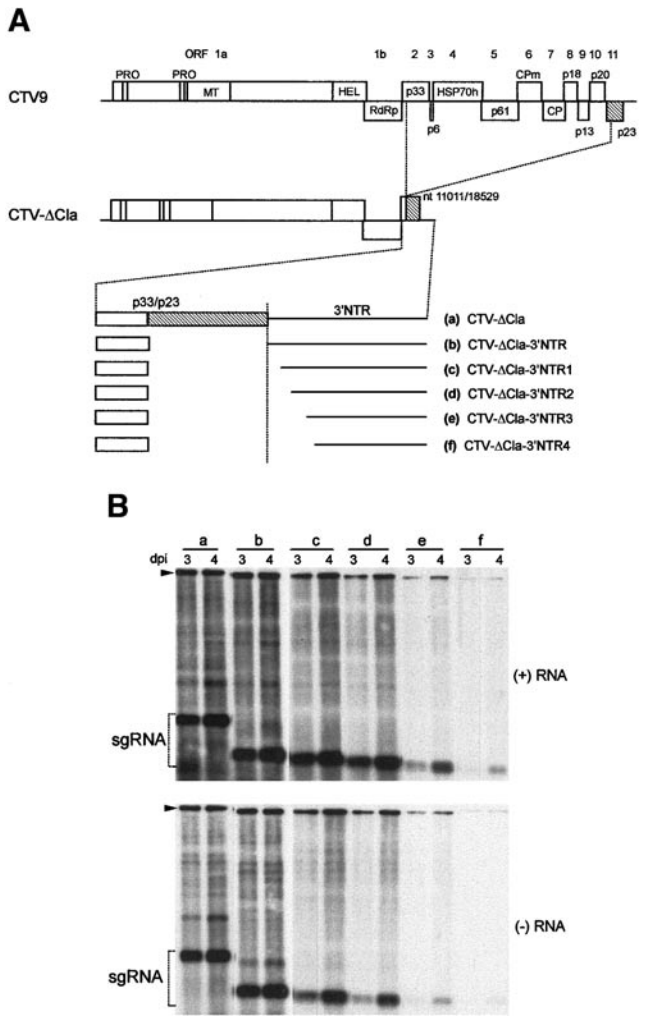

FIG. 1. Examination of minimal *cis*-acting elements in the 3′-terminus. (A) Schematic representation of the genomic organization of CTV (CTV9) and CTV replicon (CTV-ΔCla) showing the putative domains of papain-like proteases (PRO), methyltransferase (MT), helicase (HEL), and RNA-dependent RNA polymerase (RdRp) and ORFs (open boxes); the dotted lines between ORFs 2 (p33) and 11 (p23) in CTV9 indicates deleted sequence and fusion of nts 11011 and 18529 (p33/p23) in CTV-ΔCla. The bottom part shows the expanded view of ORFs 2/11 fusion (p33/p23) and 3′-NTR present in CTV-ΔCla (a). The remaining sequence of ORF 11 (p23) was deleted in CTV-ΔCla-3′NTR (Satyanarayana *et al.,* 1999) (b). Mutants with deletion of remaining sequences of p23 ORF plus 20 nts (CTV-ΔCla-3′NTR1) (c), 39 nts (CTV-ΔCla-3′NTR2) (d), 60 nts (CTV-ΔCla-3′NTR3) (e), and 66 nts (CTV-ΔCla-3′NTR4) (f) in the 5′ region of 3′-NTR; gaps represent deleted sequences. (B) Northern blot analysis of accumulation of positive- and negative-stranded genomic and sgRNAs from *N. benthamiana* protoplasts transfected with CTV-ΔCla, CTV-ΔCla-3′NTR, and deletion mutants (c–f) at 3 and 4 dpi using 3′ positive- and negative-stranded RNA-specific digoxigenin-labeled riboprobes. Position of genomic RNA is indicated by arrowheads.

We examined whether CTV could tolerate further deletions into the 3′-NTR by introducing a series of progressive deletions from the 5′ direction into the 3′-NTR. The mutants CTV-ΔCla-3′NTR1 and CTV-ΔCla-3′NTR2 had deletions of 20 and 39 nts, respectively, in the 5′ of the 3′-NTR (Fig. 1A, c, d). *In vitro*-produced RNA transcripts from CTV-ΔCla-3′NTR1 and CTV-ΔCla-3′NTR2 were used to inoculate protoplasts, and the levels of accumulation of genomic RNA at 4 days post inoculation (dpi) from the transfected protoplasts were quantified using the OS-SCAN program (Oberlin Scientific, Oberlin, OH). Deletion of 20 or 39 nts in the 5′ end of the 3′-NTR resulted in replication at levels of 50–70% and 30–50%, respectively, when compared to that of CTV-ΔCla and CTV-ΔCla-3′NTR (Fig. 1B, compare 'c' and 'd' with 'a' and 'b'), suggesting that this region of the NTR affected the efficiency of replication, but appeared not to be an integral part of the *cis*-acting elements. In contrast, mutant CTV-ΔCla-3′NTR3, which contained a deletion of 60 nts, and mutant CTV-ΔCla-3′NTR4, with a deletion of 66 nts in the 5′ region of the 3′-NTR (Fig. 1A, e, f), resulted in greatly reduced levels of replication (2–5%) (Fig. 1B, compare "e" and "f" with "a" and "b").

3′-NTRs are highly conserved among different CTV isolates

The complete nucleotide sequences of six different CTV isolates are available in the GenBank under Accession Nos. T36 (NC_001661), VT (U56902), T385 (Y18420), T30 (AF260651), SY568 (AF001623), and NUagA (AB046398). The 3′-NTRs of these CTV isolates are 273–274 nts, and sequence comparison using the ClustalW program (Thompson *et al.,* 1994) revealed ~95% identity among the isolates (Fig. 2). The multiple alignment shows that only 12 nts, distributed within the 5′ half of 3′-NTR, were not conserved among all the isolates, while the 3′ 142 nts were completely identical with the exception that NUagA was not reported to end in a terminal A (Fig. 2). This level of conservation is remarkable considering that some of these isolates differ in the 5′ half of the genome by as much as 58% (Mawassi *et al.,* 1996; López *et al.,* 1998; Albiach-Martí *et al.,* 2000). In contrast, the 3′-NTRs of the Ukranian and California isolates of the related *Beet yellows virus* (BYV) differ considerably, even with substantially different lengths, 182 and 166 nts, respectively (Agranovsky *et al.,* 1991; Peremyslov *et al.,* 1998).

Previously, we examined the compatibility of the T36 replicase complex with heterologous 3′-NTRs from isolates VT and T30 (Satyanarayana *et al.,* 1999). The 3′-NTR of T36 differs from those of T30 and VT by 8 and 6 nts, respectively, with all of the differences in the 5′ half of the 3′-NTR (Fig. 2). CTV-ΔCla-3′NTR with a T30 or VT 3′-NTR substitution replicated approximately 70% and 50%, respectively, compared to that of the homologous 3′-NTR (Satyanarayana *et al.,* 1999). The decreased replication of these mutants suggested that the 6–8 nts difference in the 5′ half of the 3′-NTRs of T30 and VT isolates affect the efficiency of replication.

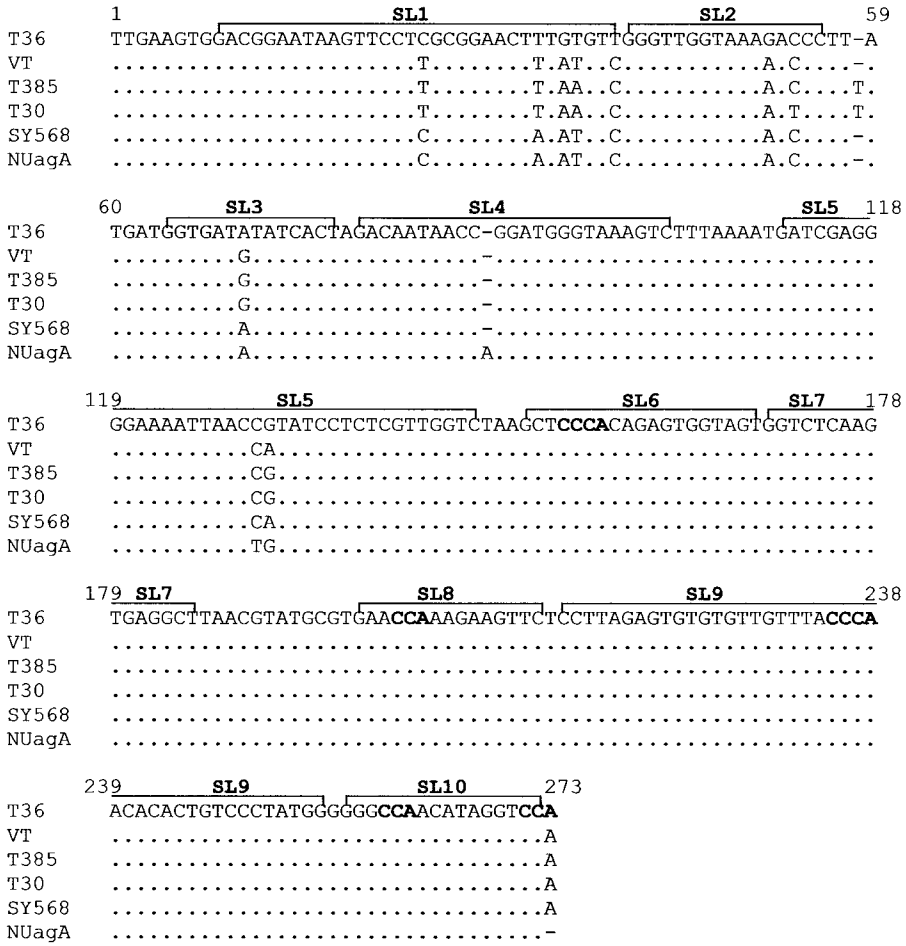

FIG. 2. Multiple alignment of the primary structure of 3′-NTR (presented as DNA) from six different CTV isolates using the ClustalW program. The GenBank Accession Nos. of sequences used in this comparison are T36: NC_001661, VT: U56902, T385: Y18420, T30: AF260651, SY568: AF001623, and NUagA: AB046398. Dots indicate the conserved nucleotides in all CTV isolates, hyphens indicate gaps introduced for optimal alignment. Only the nucleotides different at least in one isolate were indicated. The position of putative stem and loop (SL) structures conserved in all CTV isolates are marked with horizontal lines on top of the alignment (SL1 through SL10). The CCA or CCCA motifs present in 3′-NTR are shown in bold letters. The nucleotide numbers presented, from 5′ to 3′, are with respect to CTV T36 isolate 3′-NTR.

Predicted secondary structure of 3′-NTR

The higher order structures in the 3′-NTR of the different isolates of CTV (nts 19024 to 19296: numbering of CTV T36) were predicted based on the Zuker group's algorithms, thermodynamics, and databases for RNA secondary structure (http://bioinfo.math.rpi.edu/~mfold/rna) (Mathews *et al.,* 1999; Zuker *et al.,* 1999). All modeling was performed using *MFOLD,* version 3.0. The 3′-NTR of CTV T36 isolate was folded into 23 sets of predicted alternative secondary structures with 5–10 putative SLs with ΔG in the range of −73.3 to −69.7 kcal/mol. However, Fig. 3 shows one predicted secondary structure with a free energy of −72.6 kcal/mol that was common to all of the CTV isolates. It was chosen as a guide to introduce mutations. This structure contains 10 independent SL structures tentatively named SL1 to SL10 from the 5′ to the 3′ end. All of these 10 putative SL structures were stable even when the 3′-NTR was folded at 42°C. Furthermore, the 3′-NTRs were predicted to fold into a similar structure when larger sequences (400, 500, 600, 1000, and 3000 nts) were examined in *MFOLD* (data not shown).

The 3′-NTRs of other members of the genus *Closterovirus,* which vary in size from 166 to 360 nts (Karasev, 2000), also folded into 5–10 putative SL structures (data not shown). Such SL structures that function as *cis*-acting elements in the 3′-terminus are found widely among other positive-stranded RNA viruses. These include members from the alpha-, sobemo-, carmo-, and flavi-like supergroups, as well as coliphages (Adhin *et al.,* 1990; Beekwilder *et al.,* 1995; Buck, 1996; Proutski *et al.,* 1997; van Rossum *et al.,* 1997; Carpenter and Simon, 1998; Bringloe *et al.,* 1999; Turner and Buck, 1999; Koev *et al.,* 2002).

When the predicted structure of the CTV 3′-NTR was compared to differences in sequences of the different

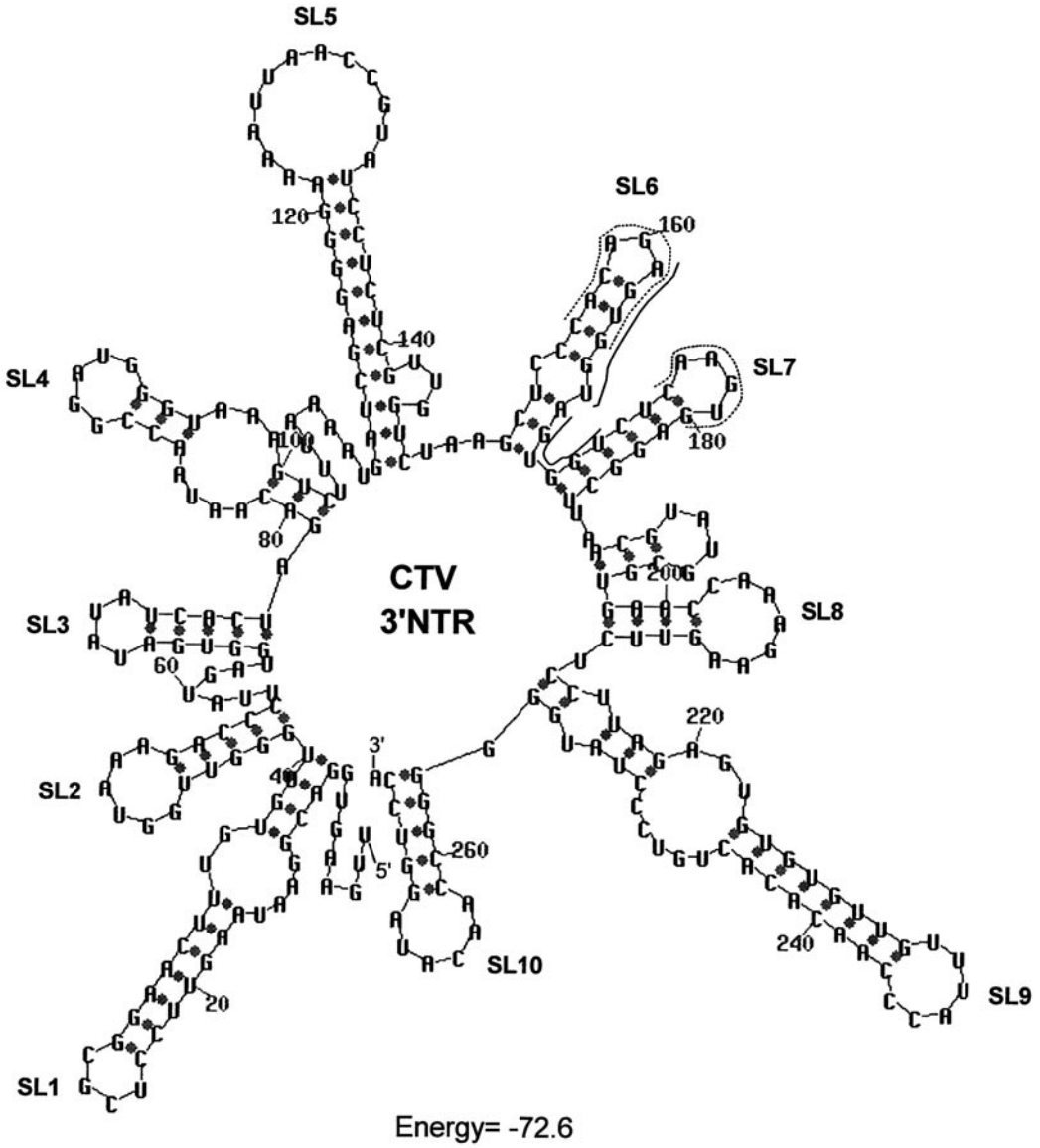

FIG. 3. The predicted secondary structure of the 3′-NTR of CTV T36 isolate using the computer structure program *MFOLD* (version 3.0) with 10 independent putative stem-and-loop (SL) structures (SL1 through SL10 from 5′ to 3′ end in 3′-NTR). The conserved nucleotides with *Beet yellows virus* are represented with broken lines around the sequence. The hexanucleotide direct repeats in SL6 and SL7 are delineated by solid lines around the sequence.

isolates, the first deviation in sequence from the 3′ end occurs in putative SL5 (Fig. 2). The first deviation in sequence between T36 and T30 was in putative SL3, and the first stem modification was in SL2. Thus, there was a remarkable conservation in sequence that composed putative SL6 through SL10 (Fig. 2). Five of the twelve nucleotide differences occur in the 5′ most SL structure (SL1). However, the mutants containing deletion of the 5′ 20 or 39 nts, which would destroy SL1, replicated at 30–70% of the wild-type level, suggesting that this area was not an integral part of the 3′ replication signal. Yet, deletion of 60 and 66 nts, which additionally removed SL2 and part of SL3, resulted in a substantial reduction in replication. Refolding of the 3′ sequences with these deletions resulted in a predicted 3′ structure almost identical to that of the wild type, suggesting that the region between nts 40 and 60, and specifically between nts 60 and 66, constitute an integral part of the 3′ replication signal.

Mutational analysis of the sequences making up putative SL structures

SL3, SL4, and SL5. Using the predicted secondary structure (Fig. 3) as a guide, we examined whether changes in the more 3′ sequence designed to alter the primary structure but to preserve the putative stem and loop secondary structures would be tolerated.

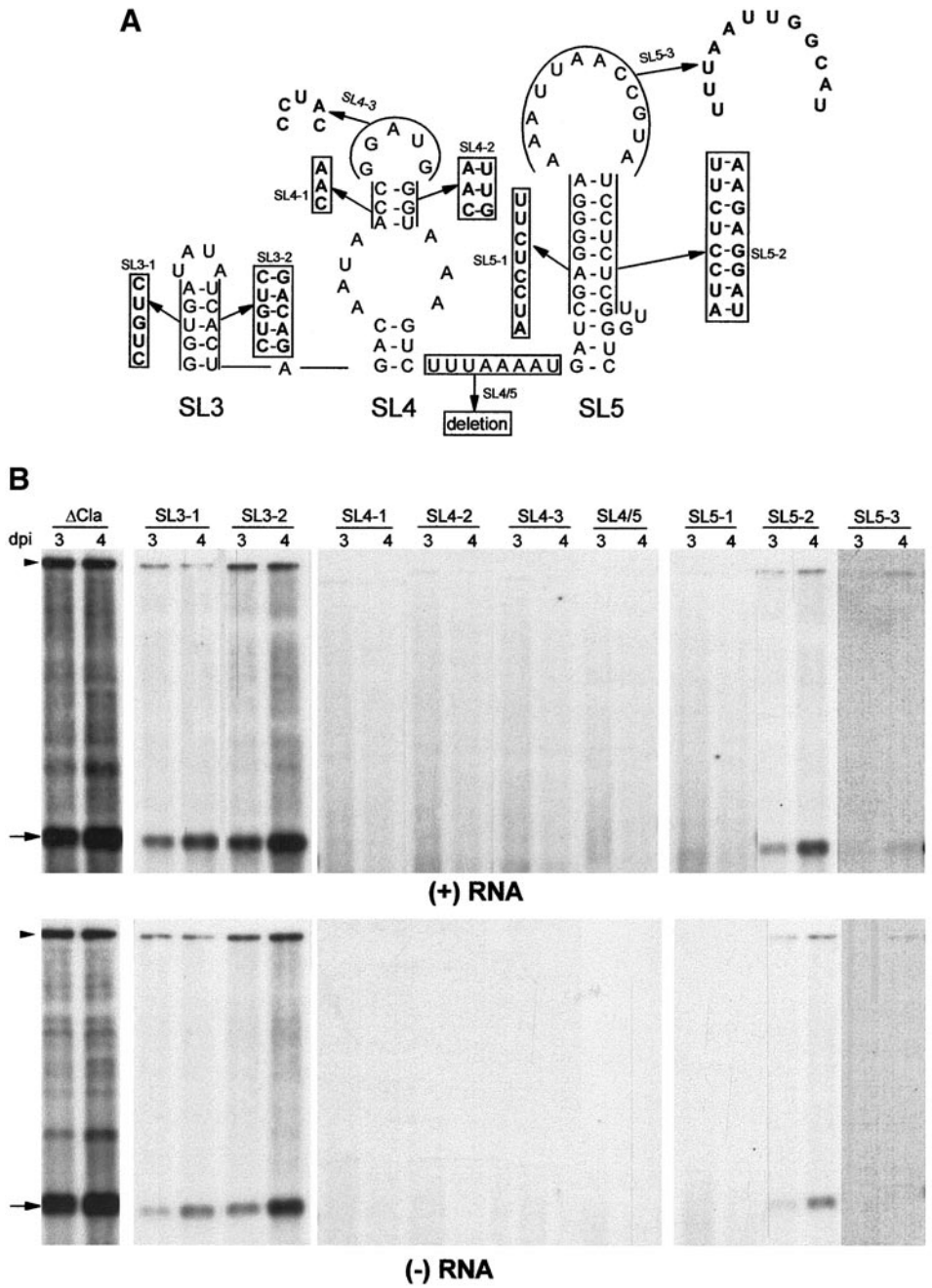

FIG. 4. Mutational analysis of putative SL3, SL4, and SL5 structures. (A) Schematic representation of mutations in putative stem-and-loop regions of predicted SL3, SL4, and SL5 structures. SL3: predicted stem structure disrupted with non-viral sequence (SL3-1) and compensatory mutations introduced into opposite side of the stem to restore the stem structure (SL3-2); SL4 and SL5: putative stem structures disrupted by replacing the left arm of stems with a nonviral sequence (SL4-1, SL5-1), the stems are restored by introducing compensatory mutations in the right arm of stems (SL4-2, SL5-2) and the loops sequence is replaced with nonviral sequences (SL4-3, SL5-3); SL4/5, sequence between SL4 and SL5 (in box) is deleted. The substituted nucleotides in the stems are boxed in boldface letters, nucleotides replaced in the loops are shown by a curved line over the sequence, and substituted nucleotides in boldface letters. (B) Northern blot analysis of mutants of SL3, SL4, and SL5 structures. The blot shows the accumulation of positive and negative-stranded RNAs from *N. benthamiana* protoplasts transfected with CTV-ΔCla and mutants of SL3, SL4 and SL5. Positions of genomic and sgRNAs are indicated by arrowheads and arrows, respectively.

Comparison of the sequence of T36 to those of VT and T30, shows that SL3 has an A to G substitution in the loop region (Figs. 2 and 3). This change was tolerated when the 3′-NTRs of VT and T30 isolates were substituted into CTV-ΔCla of T36 isolate (Satyanarayana *et al.,* 1999). To examine the putative stem structure of SL3, the sequence GGUGA, which comprises the left arm of the putative stem of SL3, was first converted to CUGUC to obtain mutant SL3-1 (Fig. 4A, SL3-1). The mutations were designed to minimize the formation of Watson-Crick base

pairs, which increase the probability of the putative stem being destabilized (Hobza and Sandorfy, 1987). Replication of mutant SL3-1 was examined by transfecting *N. benthamiana* protoplasts followed by Northern blot hybridization. SL3-1 replicated and accumulated genomic and sgRNAs, but the level of genomic RNA accumulation was estimated to be only about 10–15% of that of CTV-ΔCla (Fig. 4B, SL3-1). We next introduced compensatory mutations into the right arm of the putative stem of SL3-1 to convert the sequence UCACU to GACAG, resulting in mutant SL3-2 (Fig. 4A, SL3-2). This mutation was designed to restore base pairing in the stem, but with a sequence different from that of the wild-type virus. Mutant SL3-2 replicated approximately three- to fourfold more than SL3-1, but only 35–50% of that of CTV-ΔCla (Fig. 4B, SL3-2). Extensive mutation of this putative stem sequence with a non-viral sequence substantially reduced replication, while restoration of the stem resulted in increased replication. In fact, mutant SL3-2 has 10 nts difference from the wild-type virus compared to only one nt variation among the different natural isolates in this region. These data suggest that the predicted secondary structure of SL3 has an important role in the 3′-replication signal.

The sequence comprising putative SL4 is completely conserved in all of the CTV isolates with the exception of a single nucleotide insertion in the loop region of NUagA isolate (Fig. 2). The requirement of sequence and/or predicted secondary structure of SL4 for replication was examined by introducing a non-viral sequence in the left arm of the top stem (mutant SL4-1, ACC to CAA), followed by compensatory mutations designed to restore the putative stem structure (mutant SL4-2, GGU to UUG); the sequence in the loop was changed with a nonviral sequence (mutant SL4-3, GGAUG to CCUAC) (Fig. 4A, SL4). The bottom stem of SL4 was not analyzed because only the top stem was stable when 3′-NTR was modeled at higher temperatures (data not shown). All mutations in this region were lethal, suggesting that the primary structure in putative SL4 is an integral part of the *cis*-acting elements for replication (Fig. 4B, SL4-1 to -3). However, the sequence designed to recreate the upper stem of SL4 did not fold into a similar SL when refolded by *MFOLD*.

The sequence comprising putative SL5 has two variable nucleotides in the loop region when comparing the CTV isolates (Figs. 2 and 3). Three mutants were generated in SL5 (Fig. 4A, SL5). In mutant SL5-1, the left arm was replaced with a non-viral sequence to disrupt the formation of the stem (CGAGGGGA to AUCCUCUU). The right arm sequence UCCUCUCG was changed to AAGAGGAU to restore the stem structure in mutant SL5-2, and the loop sequence AAAUUAACCGUA was replaced with UUUAAUUGGCAU to generate mutant SL5-3 (Fig. 4A, SL5). Disruption of the stem was lethal (Fig. 4B, SL5-1); however, compensatory mutations in SL5-2 partially restored the replication (7–15% compared to that of CTV-ΔCla) (Fig. 4B, SL5-2), suggesting that the secondary structure was needed for replication. The substitution of the loop sequence with a nonviral sequence in mutant SL5-3 resulted in replication only at barely detectable levels (~2% compared to that of CTV-ΔCla), suggesting the requirement of primary structure for efficient replication (Fig. 4B, SL5-3). Substantial mutation of the putative stem regions of SL5 with nonviral sequences was tolerated. Although mutations that disrupted the stem were lethal, a compensatory mutation to rebuild the stem with a total of 16 nonviral nts resulted in continued replication, compared to only two variable nts among the natural isolates. Changes in the primary structure in the region of SL5 was tolerated more than those in the SL4 region.

To examine whether the sequence between the SL4 and SL5 regions could be deleted without affecting the replication level, mutant SL4/5 was generated by deleting the sequence UUUAAAAU between putative structures SL4 and SL5 (Fig. 4A, SL4/5). Although mutant SL4/5 could be folded into similar stem-and-loop structures as the wild-type RNA, it failed to replicate to detectable levels in protoplasts (Fig. 4B, SL4/5).

SL6, SL7, and SL8. The sequences in regions SL6, SL7, and SL8 were completely conserved among all CTV isolates (Fig. 2). Mutant SL6-1, with the sequence GUGGUAGU, which comprises the right arm of the putative stem converted into UGUAUCUA, failed to replicate at detectable levels (Fig. 5, SL6-1). We observed a 6 nts direct repeat sequence, AGUGGUAGUGGU, overlapping the predicted structures SL6 and SL7 (Fig. 3). It is possible that failure of SL6-1 to replicate was the result of disruption of this directly repeated sequence. To examine this possibility, the left arm sequence GCUCCCAC was replaced with a nonviral sequence (UAGCUACA), keeping the direct repeat sequence intact, but disrupting the formation of the stem (Fig. 5A, SL6-2). This mutant, SL6-2, also failed to replicate to detectable levels (Fig. 5B, SL6-2). We next introduced compensatory mutations into the left arm of the putative stem structure to convert the sequence GCUCCCAC in SL6-1 to UAGCUACA, resulting in mutant SL6-3 (Fig. 5A, SL6-3). The inability of this mutation to restore replication in protoplasts suggested that primary structure of putative SL6 was needed for replication or that our compensatory mutations did not create an equivalent secondary structure (Fig. 5B, SL6-1 to -3). The sequence AGA in SL6 loop was changed to CAU to obtain mutant SL6-4 (Fig. 5A, SL6-4). This mutant was able to replicate at 5–10% of that of CTV-ΔCla (Fig. 5B, SL6-4), suggesting that the sequence of the putative loop region is important for efficient replication but is somewhat flexible.

The SL7 region was analyzed by changing the left arm sequence, GGUCUC, in the predicted stem with CAAACA, resulting in mutant SL7-1 (Fig. 5A, SL7-1). This mutant failed to replicate to detectable levels (Fig. 5B,

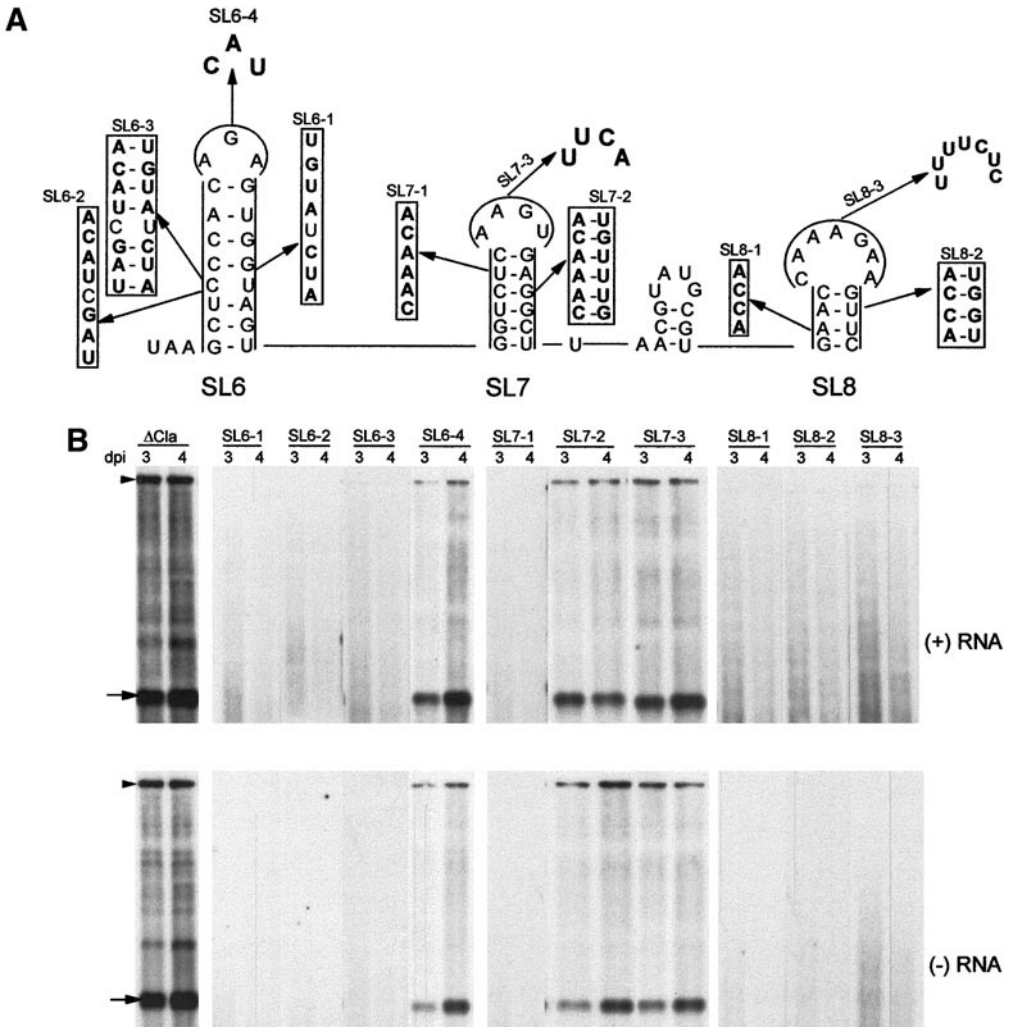

FIG. 5. Examination of the requirement of SL6, SL7, and SL8 by mutational analysis. (A) Schematic representation of putative SL6, SL7, and SL8 structures in the 3′-NTR. Mutated nucleotides in putative stems are shown with vertical lines and nucleotides that are substituted into stems are boxed in boldface letters; curves around the loop regions indicate the nucleotides that are replaced with nonviral sequence (in boldface). The names of the mutants are indicated above the sequence. (B) Northern blot analysis of accumulation of positive- and negative-stranded RNAs from SL6, SL7, and SL8 mutants transfected protoplasts at 3 and 4 dpi. Positions of genomic and sgRNAs are indicated by arrowheads and arrows, respectively.

SL7-1). We attempted to restore the stem structure by introducing compensatory mutations in the right arm of the putative stem by changing the sequence GAGGCU in SL7-1 to UGUUUG, resulting in mutant SL7-2 (Fig. 5A, SL7-2). This mutant restored the replication at the level of 10–15% when compared to that of CTV-ΔCla, suggesting involvement of the predicted secondary structure in replication (Fig. 5B, SL7-2). The sequence AAGU in the loop of SL7 was replaced with UUCA to obtain SL7-3 (Fig. 5A, SL7-3). This mutant replicated at 15–20% of the level of CTV-ΔCla, demonstrating tolerance for mutation in this region (Fig. 5B, SL7-3).

Three mutants were generated to examine the region encompassing the predicted structure SL8. The sequence GAAC in the left arm was changed to ACCA to obtain mutant SL8-1 (Fig. 5A, SL8-1). Compensatory mutations were introduced into the right arm to restore the stem structure (GUUC to UGGU), resulting in mutant SL8-2 (Fig. 5A, SL8-2). Finally, the loop sequence CAAA-GAA was replaced with UUUUCUC to obtain mutant SL8-3 (Fig. 5A, SL8-3). All three mutations abolished detectable levels of replication, demonstrating the importance of primary structure of the predicted SL8 region for replication (Fig. 5B, SL8-1 to -3).

Pair-wise comparison of CTV and BYV 3′-NTRs revealed two conserved regions of nine (CACAGAGUG) and six (CAAGUG) nts in the upper part of putative SL6 and SL7, respectively (Fig. 3). Since mutations in these conserved regions in CTV substantially decreased the levels of replication, it is possible that these conserved sequences in BYV also play an important role as *cis*-acting elements.

SL9 and SL10. To examine the SL9 region, three mutants were generated. Mutant SL9-1 was produced by

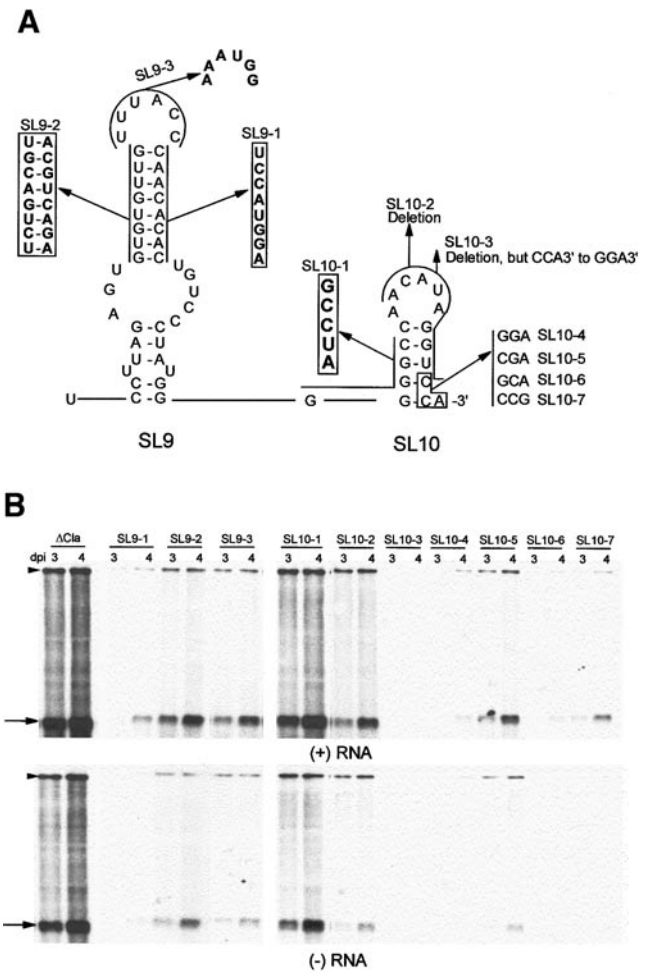

FIG. 6. Mutational analysis of putative SL9 and SL10 structures. (A) Schematic representation of the predicted SL9 and SL10 structures. SL9: stem disruption (SL9-1), compensatory mutations (SL9-2) with nonviral sequence, and substitution of loop with nonviral sequence (SL9-3); SL10: change at the left arm of stem to disrupt the putative stem (SL10-1), deletion of right arm and loop sequence that ends with CCA-3′ (SL10-2) or GGA-3′ (SL10-3), mutations in 3′ triplet CCA to GGA (SL10-4), CGA (SL10-5), GCA (SL10-6) or CCG (SL10-7). Mutated nucleotides in stems are shown with lines, and nucleotides that are substituted into the stems are boxed in boldface letters; replaced nucleotides with nonviral sequence (in boldface letters) in loops are shown with curved lines. The 3′ triplet is boxed. (B) Northern blot hybridization of SL9 and SL10 mutants. The blot shows the accumulation of plus- and minus-stranded RNAs from SL9 and SL10 mutants transfected protoplasts at 3 and 4 dpi. Arrowheads and arrows represent the position of genomic and sgRNAs, respectively.

replacing the sequence CAACACAC in the right arm of the top stem with the nonviral sequence UCCAUGGA, to disrupt the formation of the putative stem structure (Fig. 6A, SL9-1). This mutation resulted in barely detectable replication, 2–5% of that of CTV-ΔCla (Fig. 6B, SL9-1). We next examined whether recreation of the predicted stem structure in SL9-1 would restore the replication. The sequence GUGUGUUG in the left arm of the top stem in mutant SL9-1 was changed to UCUGACGU in mutant SL9-2 (Fig. 6A, SL9-2). The compensatory mutations in mutant SL9-2 resulted in an ~four- to fivefold increase in replication when compared to mutant SL9-1 (Fig. 6B, SL9-2). Despite this increase, replication of SL9-2 was only 10–20% of that of CTV-ΔCla. The third mutant, SL9-3, was obtained by changing the loop sequence of SL9 with a nonviral sequence (Fig. 6A, SL9-3). This mutant replicated at 5–10% of the level of CTV-ΔCla (Fig. 6B, SL9-3). In contrast to SL8, the putative SL9 region tolerated considerable changes in the predicted stem and loop regions. Substitution of eight nonviral nts to disrupt the putative stem resulted in reduced, but continued replication. Substitution of an additional eight nonviral nts to reconstruct the stem structure resulted in increased replication even though this was a substitution of 16 nonviral nts in a region that has no variation among CTV isolates. These data suggest that both primary and the predicted secondary structure are involved in optimal replication.

The requirement of SL10 was examined by replacing the sequence GGGGC at the left arm of SL10 with a nonviral sequence AUCCG, resulting in mutant SL10-1 (Fig. 6A, SL10-1). This mutant replicated at 40–50% of the level of CTV-ΔCla, indicating that mutations designed to disrupt the stem of putative SL10 only marginally affected replication efficiency (Fig. 6B, SL10-1). We then deleted the 3′-most 11 nts (ACAUAGGUCCA) to terminate the RNA with CCA, the normal 3′ triplet in wild-type virus (Fig. 6A, SL10-2). This mutant, SL10-2, had a deletion of the right arm of putative SL10 and most of the loop sequence. However, this deletion resulted in a reduced but significant level of replication, 15–20% of that of CTV-ΔCla (Fig. 6B, SL10-2). It is remarkable that replication continued with the deletion of the 3′-most 11 nts that comprised part of putative SL10. The 3′-terminal SL structures present in *Turnip crinkle virus* (TCV) and *Barley yellow dwarf virus* were found to be essential for *in vitro* and *in vivo* functions (Song and Simon, 1995; Koev *et al.,* 2002).

Thus, the region of putative SL10 appeared to be even more flexible than SL9. Alteration of five nucleotides at the left arm of the putative stem had little effect on replication. Replication continued even with deletion of the loop and the right arm of the stem. Both regions, SL9 and SL10, were unusually tolerant to mutations even though these regions are totally conserved among the CTV isolates. It is possible that this sequence is not an important part of the 3′ replication signal, but is maintained by selection based on the efficiency of replication, or perhaps it provides some function that is required for the virus-host interaction in plants but not in protoplasts.

In contrast to the other reported sequences, the sequence of the NUagA isolate does not end with the 3′ triplet CCA. We examined the *in vivo* role of 3′ triplet by replacing CCA-3′ with GGA (SL10-4), CGA (SL10-5), GCA (SL10-6), or CCG (SL10-7) (Fig. 6A, SL10). All of the substitutions for the last three nucleotides resulted in much reduced levels of replication, 2–15% of that of CTV-ΔCla,

suggesting an important role for 3′ terminus CCA nucleotides in replication (Fig. 6B, SL10-4 to -7). We further examined the 3′ triplet by replacing the CCA with GGA in SL 10-2, the mutant with the 3′ eleven nts deleted, creating SL10-3 (Fig. 6, SL10-3). This mutant also replicated at barely detectable levels, suggesting that the 3′ triplet, CCA, was needed to initiate replication (Fig. 6B, SL10-3). Thus, the common theme of a requirement for a 3′ terminal CC(A/G) motif for many plant RNA viruses (Dreher, 1999) appears to be continued in this group of largest and most complex plant viruses. It was interesting to note the presence of CCA or CCCA motifs at five different locations in the 3′-NTR of CTV (Fig. 2). The RdRps of Qβ, *Turnip yellow mosaic virus,* and TCV were able to initiate minus-strand synthesis from internal $C_{2\text{-}4}A$ repeats present in short linear RNAs (Yoshinari and Dreher, 2000; Yoshinari *et al.,* 2000; Tretheway *et al.,* 2001). One function of secondary structure appears to be to make internal CC(A/G) motifs inaccessible (Singh and Dreher, 1998). CTV can initiate RNA synthesis from an upstream CCA when it is at the 3′ terminus. However, there is no evidence that CTV initiates internally *in vivo.* In fact, all of the internal motifs appear to be in a duplex structure, perhaps making them inaccessible for minus-strand initiation. However, in the structure shown in Fig. 3, even the terminal motif is mostly in a duplex structure.

It should be noted that the *Xho*I restriction site in the cDNA template was engineered to generate run-off *in vitro* transcripts that resulted in an additional 'C' residue in the extreme 3′ end in all the mutants. However, additional nts at the 3′ terminus of *in vitro* transcripts often do not negatively affect infectivity. For example, wild-type TMV tolerated up to seven extra nucleotides in the 3′ terminus without significant loss of infectivity (Dawson *et al.,* 1986). Since initiation is thought to occur opposite the 3′ C within the CC(A/G) initiation box (Dreher, 1999), as long as the initiation box is accessible the extra 3′ nts should be irrelevant.

BYV 3′-NTR is noncompatible with CTV replicase complex

Previously, it was shown that among the members of *Bromoviridae* and *Tobamoviridae* the compatibility of the replicase complex with the 3′ replication signals was extended to heterologous 3′-NTRs from related viruses (Pacha and Ahlquist, 1991; Rao and Grantham, 1994; Donson *et al.,* 1991; Shivprasad *et al.,* 1999; Chandrika *et al.,* 2000), and even tandem 3′-NTRs (Hilf and Dawson, 1993). Since 3′-NTRs from different strains of CTV are compatible with the T36 replicase complex in CTV-ΔCla-3′NTR (Satyanarayana *et al.,* 1999), we examined whether the heterologous 3′-NTR from a different closterovirus, BYV, is compatible with the CTV replicase complex. The 166 nt 3′-NTR of BYV-California isolate (Peremyslov *et al.,* 1998) has 46% nucleotide identity with CTV

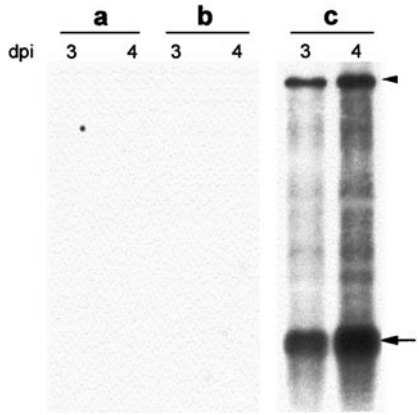

FIG. 7. Replication of CTV hybrid containing BYV 3′-NTR. CTV-ΔCla-BYV3′NTR contains precise exchange of BYV 3′-NTR into CTV-ΔCla-3′NTR. The Northern blot shows the accumulation of positive stranded RNAs from CTV-ΔCla-BYV3′NTR (a and b; two independent clones) and CTV-ΔCla (c) transfected *N. benthamiana* protoplasts at 3 and 4 dpi. CTV-ΔCla-BYV3′NTR probed with BYV 3′ end positive-stranded RNA specific-digoxigenin labeled riboprobe, and CTV-ΔCla probed with CTV 3′ terminal positive-stranded RNA specific digoxigenin labeled probe. Position of the genomic and sgRNAs are indicated with an arrowhead and an arrow, respectively.

3′-NTR. The BYV 3′-NTR was folded into 3 alternative predicted secondary structures with 5–6 putative SLs. The 3′-NTR of BYV was PCR amplified from pBYV-NA (Peremyslov *et al.,* 1998) and substituted into pCTV-ΔCla to obtain pCTV-ΔCla-BYV3′NTR. This mutant failed to replicate to detectable levels (Fig. 7), suggesting that the recognition of heterologous 3′ replication signals does not extend to other closteroviruses.

CONCLUSION

The members of the *Closteroviridae* do not contain well-defined 3′ structures such as the tRNA-mimics or a poly A region; instead, the 3′ region required for replication appears to consist of a series of SL structures. However, we were not able to predict possible higher order structures such as pseudoknots, kissing stem-loops, or long distance interactions. The highly conserved 3′-NTRs of different CTV isolates were folded into a common complex structure with 10 SLs. The results of mutational analysis of the putative SL structures suggest that some regions were more integral to the 3′ replication signal than others; the secondary structures of some potential SLs appeared to be involved in replication, while primary structures were more important in other areas (Fig. 8). Secondary structures of SL3, SL5, SL7, and SL9 are probably biologically significant, whereas, mutations in SL4, SL6, and SL8 demonstrated importance of primary structures. SL1, SL2, SL3, and SL10 allowed considerable deletion with continued replication, suggesting that these regions were not essential for basal-level replication, but appear to be required for efficient

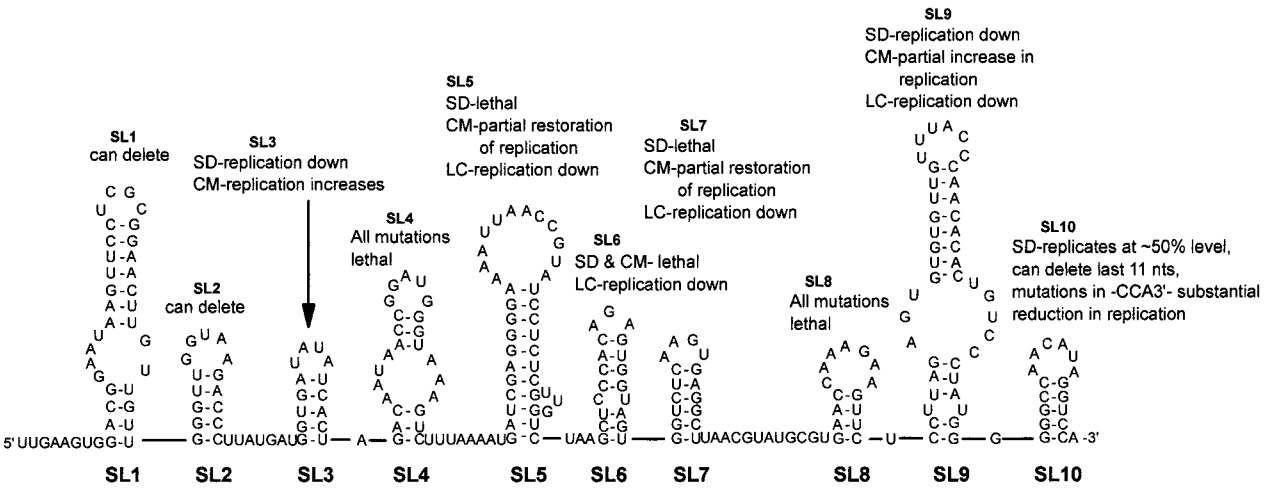

FIG. 8. Schematic representation of the proposed secondary structure of the 3′-NTR of CTV T36 isolate with 10 independent putative stem-and-loop (SL) structures from the 5′ to 3′ end. The summary of mutational analysis in SL structures is indicated on top of the respective SLs. SD, stem disruption with nonviral sequence; CM, compensatory mutations to restore the putative stem structure with nonviral sequence; LC, loop change with non-viral sequence.

replication, while the central areas (SL4, SL6, and SL8) appeared to be integral components of the replication signal. It is somewhat unusual that the 3′-most regions, comprising SL9 and SL10, allowed considerable mutagenesis and even deletion of the last eleven nts. We examined the 3′ sequences required for replication of CTV in protoplasts, which likely involves an aggregate of functions, including minus-strand initiation, replicase specificity, regulation of translation, stability of RNA, and inhibition of negative-strands late in infection. At this time, we cannot identify sequences or structures involved in any specific functions.

A basic function of the 3′ terminus is minus-strand initiation. In this context, CTV may be more complicated than simpler RNA viruses because it produces unusually large amounts of negative strands of both genomic and sgRNAs (Satyanarayana *et al.,* 2002). Additionally, minus-strand initiation might be a point of regulation of both genomic and sgRNA syntheses. We have been unable to determine whether the ten sgRNAs that serve as messengers for the 3′ genes are produced from the genomic RNA by promotion internally from negative strands or by termination internally during negative-strand synthesis and, also, whether the sgRNAs are transcribed from complementary sgRNAs (Gowda *et al.,* 2001). Thus, there may be a need for discretion of initiation at 3′ ends of genomic versus sgRNAs. Additionally, we have shown that the p23 gene regulates asymmetry of positive to negative strands of both genomic and sgRNAs (Satyanarayana *et al.,* 2002). In the absence of p23, negative-stranded RNA synthesis continues to near unity with positive strands. It is possible that one function of the 3′ replication signal is to bind p23, perhaps making the 3′ minus-strand promoter unavailable.

MATERIALS AND METHODS

Generation of 3′-NTR mutants

The cDNA clones of CTV replicons pCTV-ΔCla and pCTV-ΔCla-3′NTR were described previously (Satyanarayana *et al.,* 1999). The nucleotide numbering and sequence of the oligonucleotides used in this investigation are according to Pappu *et al.* (1994) and Karasev *et al.* (1995), GenBank Accession No. NC_001661. Infectious cDNA clone, pCTV9 (Satyanarayana *et al.,* 1999), was used as a template in all polymerase chain reactions (PCR) with either Pfu DNA polymerase (Stratagene, La Jolla, CA) or Vent DNA polymerase (New England Biolabs, Beverly, MA). CTV-ΔCla-3′NTR1 to 4 were generated by PCR amplifying various lengths of 3′-NTR using a pair of oligonucleotides that contained *Cla*I and *Not*I restriction endonuclease sites in the forward and reverse primers, respectively. The PCR products were ligated into CTV-ΔCla between *Cla*I and *Not*I restriction sites, thus deleting the remaining sequence of p23 ORF plus various lengths in the 5′ region of 3′-NTR (Fig. 1A).

Mutations with nonviral sequences that disrupted putative stems, compensatory mutations to restore the stem structures, and change of loop sequences in SL3 to SL9 were introduced by PCR using mutagenized oligonucleotides, followed by overlap-extension PCR (Ho *et al.,* 1989) of the region between nts18529 and 19296 that contained *Cla*I, and *Xho*I and *Not*I restriction sites at the 5′ and 3′ end of PCR products, respectively. The *Cla*I and *Not*I digested PCR products were directly ligated into similarly digested pCTV-ΔCla. The positive clones were screened for the presence of the *Xho*I restriction site. Mutations in putative SL10 and extreme 3′-terminal CCA nucleotides were generated by PCR amplifying a DNA

fragment between nts 18529 and 19296 using mutagenized reverse primers that contained *Xho*I and *Not*I restriction sites. The PCR amplified products were ligated into pCTV-ΔCla between *Cla*I and *Not*I restriction sites.

The 3′-NTR of BYV was PCR amplified from pBYV-NA (Peremyslov *et al.,* 1998) using specific primers with *Cla*I and *Not*I restriction sites at the 5′ and 3′ ends, respectively. The PCR product was ligated into pCTV-ΔCla between *Cla*I and *Not*I sites, thus replacing the remaining sequence of the p23 ORF and the 3′-NTR of CTV with the BYV 3′-NTR.

All the mutations were confirmed by DNA sequencing. Mutations that were introduced to restore the stem structure and change of loop sequence retained the predicted secondary structures when examined by *MFOLD* program.

Protoplasts transfection and analysis of viral RNAs

Isolation of mesophyll protoplasts from *N. benthamiana* and polyethylene glycol-mediated transfections were carried out as described in Satyanarayana *et al.* (1999). The capped *in vitro* transcripts were generated from *Not*I- or *Xho*I-linearized plasmid DNAs using SP6 RNA polymerase (Epicentre Technologies, WI) as described in Satyanarayana *et al.* (1999). Freshly prepared *in vitro* transcripts in 30 μl volumes were used to directly inoculate $\sim 1 \times 10^6$ mesophyll protoplasts. Total nucleic acids from 3 and 4 dpi protoplasts were isolated and analyzed by Northern blot hybridization as described previously (Satyanarayana *et al.,* 1999). The 3′-terminal 900 nts of CTV T36 in pGEM-7Zf (Promega) were used to generate positive- and negative-stranded RNA-specific riboprobes with digoxigenin-labeled UTP using either SP6 or T7 RNA polymerase. The positive- and negative-stranded-RNA specific probes were equalized using double-stranded RNAs extracted from CTV T36-infected plants as described in Satyanarayana *et al.* (2002). The relative levels of replication of the mutants were quantified by scanning and densitometry of the genomic RNA bands at 4 dpi using different exposures of Northern blots with the OS-SCAN program (Oberline Scientific, Oberlin, Ohio). Results presented represent at least four to five independent protoplasts transfections using two to three independent clones for each mutant.

ACKNOWLEDGMENTS

We thank Theo Dreher for useful discussion and critical reading of the manuscript, and John Cook, Cecile Robertson, and Judy Harber for excellent technical assistance. This research was supported in part by an endowment from the J. R. and Addie S. Graves family and grants from the Florida Citrus Production Research Advisory Council, the National Citrus Research Council, the U.S.-Israel Binational Agricultural Research and Development Fund, USDA/ARS Cooperative Agreement, the USDA/NRI, and the Florida Agricultural Experiment Station, and approved for publication as Journal Series No. R-08741.

REFERENCES

Adhin, M. R., Alblas, J., and van Duin, L. (1990). Secondary structure at the 3′-terminal region of RNA coliphages: Comparison with tRNA. *Biochim. Biophys. Acta.* **1050,** 110–118.

Agranovsky, A. A., Boyko, V. P., Karasev, A. V., Lunina, N. A., Koonin, E. V., and Dolja, V. V. (1991). Nucleotide sequence of the 3′-terminal half of beet yellows closterovirus RNA genome: unique arrangement of eight virus genes. *J. Gen. Virol.* **72,** 15–23.

Albiach-Martí, M. R., Mawassi, M., Gowda, S., Satyanarayana, T., Hilf, M. E., Shanker, S., Almira, E. C., Vives, M. C., López, C., Guerri, J., Flores, R., Moreno, P., Garnsey, S. M., and Dawson, W. O. (2000). Sequences of citrus tristeza virus separated in time and space are essentially identical. *J. Virol.* **74,** 6856–6865.

Beekwilder, M. J., Nieuwenhuizen, R., van Duin, J. (1995). Secondary structure model for the last two domains of single-stranded RNA phage Q beta. *J. Mol. Biol.* **247,** 903–917.

Bringloe, D., Pleij, C. W. A., and Coutts, R. H. A. (1999). Mutation analysis of *cis*-elements in the 3′- and 5′-untranslated regions of satellite tobacco necrosis virus strain C RNA. *Virology* **264,** 76–84.

Buck, K. W. (1996). Comparison of the replication of positive-stranded RNA viruses of plants and animals. *Adv. Virus Res.* **47,** 159–251.

Carpenter, C. D., and Simon, A. E. (1998). Analysis of sequences and predicted structures required for viral satellite RNA accumulation by *in vivo* genetic selection. *Nucleic Acids Res.* **26,** 2426–2432.

Chandrika, R., Rabindran, S., Lewandowski, D. J., Manjunath, K. L., and Dawson, W. O. (2000). Full-length tobacco mosaic virus RNAs and defective RNAs have different 3′ replication signals. *Virology* **273,** 198–209.

Chapman, M. R., and Kao, C. C. (1999). A minimal RNA promoter for minus-strand RNA synthesis by the brome mosaic virus polymerase complex. *J. Mol. Biol.* **286,** 709–720.

Dawson, W. O., Beck, D. L., Knorr, D. A., and Grantham, G. L. (1986). cDNA cloning of the complete genome of tobacco mosaic virus and production of infectious transcripts. *Proc. Natl. Acad. Sci. USA* **83,** 5043–5047.

Dolja, V. V., Karasev, A. V., and Koonin, E. V. (1994). Molecular biology and evolution of closteroviruses: sophisticated build-up of large RNA genomes. *Ann. Rev. Phytopathol.* **32,** 261–285.

Donson, J., Kearney, C. M., Hilf, M. E., and Dawson, W. O. (1991). Systemic expression of a bacterial gene by a tobacco mosaic virus-based vector. *Proc. Natl. Acad. Sci. USA* **88,** 7204–7208.

Dreher, T. W. (1999). Functions of the 3′-untranslated regions of positive strand RNA viral genomes. *Annu. Rev. Phytopathol.* **37,** 151–174.

Duggal, R., Lahser, F. C., and Hall, T. C. (1994). *Cis*-acting sequences in the replication of plant viruses with plus-sense RNA genomes. *Ann. Rev. Phytopathol.* **32,** 287–309.

Febres, V. J., Ashoulin, L., Mawassi, M., Frank, A., Bar-Joseph, M., Manjunath, K. L., Lee, R. F., and Niblett, C. L. (1996). The p27 protein is present at one end of citrus tristeza virus particles. *Phytopathology* **86,** 1331–1335.

Gowda, S., Satyanarayana, T., Davis, C. L., Navas-Castillo, J., Albiach-Martí, M. R., Mawassi, M., Valkov, N., Bar-Joseph, M., Moreno, P., and Dawson, W. O. (2000). The p20 gene product of citrus tristeza virus accumulates in the amorphous inclusion bodies. *Virology* **274,** 246–254.

Gowda, S., Satyanarayana, T., Ayllón, M. A., Albiach-Martí, M. R., Mawassi, M., Rabindran, S., Garnsey, S. M., and Dawson, W. O. (2001). Characterization of the *cis*-acting elements controlling subgenomic mRNAs of citrus tristeza virus: production of positive- and negative-stranded 3′-terminal and positive-stranded 5′-terminal RNAs. *Virology* **286,** 134–151.

Hilf, M. E., and Dawson, W. O. (1993). The tobamovirus capsid protein functions as a host-specific determinant of long distance movement. *Virology* **193,** 106–114.

Hilf, M. E., Karasev, A. V., Pappu, H. R., Gumpf, D. J., Niblett, C. L., and

Garnsey, S. M. (1995). Characterization of citrus tristeza virus subgenomic RNAs in infected tissue. *Virology* **208,** 576–582.

Ho, S. N., Hunt, H. D., Horton, R. M., Pullen, J. K., and Pease, L. R. (1989). Site-directed mutagenesis by overlap extension using polymerase chain reaction. *Gene* **77,** 51–59.

Hobza, P., and Sandorfy, C. (1987). Nonempirical calculation on all the 29 possible DNA base pairs. *Biochemistry* **109,** 1302–1307.

Karasev, A. V., Boyko, V. P., Gowda, S., Nikolaeva, O. V., Hilf, M. E., Koonin, E. V., Niblett, C. L., Cline, K., Gumpf, D. J., Lee, R. F., Garnsey, S. M., Lewandowski, D. J., and Dawson, W. O. (1995). Complete sequence of the citrus tristeza virus RNA genome. *Virology* **208,** 511–520.

Karasev, A. V. (2000). Genetic diversity and evolution of closteroviruses. *Annu. Rev. Phytopathol.* **38,** 293–324.

Kim, C. H., Kao, C. C., and Tinoco, I., Jr. (2000). RNA motifs that determine specificity between a viral replicase and its promoter. *Nat. Struct. Biol.* **7,** 415–423.

Koev, G., Liu, S., Beckett, R., and Miller, W. A. (2002). The 3′-terminal structure required for replication of barley yellow dwarf virus RNA contains an embedded 3′ end. *Virology* **292,** 114–126.

Koonin, E. V., and Dolja, V. V. (1993). Evolution and taxonomy of positive-strand RNA viruses: implications of comparative analysis of amino acid sequences. *Crit. Rev. Biochem. Mol. Biol.* **28,** 375–430.

Lai, M. M. C. (1998). Cellular factors in the transcription and replication of viral RNA genomes: A parallel to DNA-dependent RNA transcription. *Virology* **244,** 1–12.

López, C., Ayllón, M. A., Navas-Castillo, J., Guerri, J., Moreno, P., and Flores, R. (1998). Molecular variability of the 5′- and 3′-terminal regions of citrus tristeza virus RNA. *Phytopathology* **88,** 685–691.

Mathews, D. H., Sabina, J., Zuker, M., and Turner, D. H. (1999). Expanded sequence dependence of thermodynamic parameters provides robust prediction of RNA secondary structure. *J. Mol. Biol.* **288,** 911–940.

Mawassi, M., Mietkiewska, E., Gofman, R., Yang, G., and Bar-Joseph, M. (1996). Unusual sequence relationships between two isolates of citrus tristeza virus. *J. Gen. Virol.* **77,** 2359–2364.

Osman, T. A. M., Hemenway, C. L., and Buck, K. W. (2000). Role of the 3′ tRNA-like structure in tobacco mosaic virus minus-strand RNA synthesis by the viral RNA-dependent RNA polymerase *in vitro*. *J. Virol.* **74,** 11671–11680.

Pacha, R. F., and Ahlquist, P. (1991). Use of bromovirus RNA3 hybrids to study template specificity in viral RNA amplification. *J. Virol.* **65,** 3693–3703.

Pappu, H. R., Karasev, A. V., Anderson, E. J., Pappu, S. S., Hilf, M. E., Febres, V. J., Eckloff, R. M. G., McCaffery, M., Boyko, V., Gowda, S., Dolja, V. V., Koonin, E. V., Gumpf, D. J., Cline, K. C., Garnsey, S. M., Dawson, W. O., Lee, R. F., and Niblett, C. L. (1994). Nucleotide sequence and organization of eight 3′ open reading frames of the citrus tristeza closterovirus genome. *Virology* **199,** 35–46.

Peremyslov, V. V., Hagiwara, Y., and Dolja, V. V. (1998). Genes required for replication of the 15.5-kilobase RNA genome of a plant closterovirus. *J. Virol.* **72,** 5870–5876.

Proutski, V., Gould, E. A., and Holmes, E. (1997). Secondary structure of the 3′ untranslated region of flaviviruses: similarities and difference. *Nucleic Acids Res.* **25,** 1194–1202.

Rao, A. L. N., and Grantham, G. L. (1994). Amplification *in vivo* of brome mosaic virus RNAs bearing 3′ noncoding regions from cucumber mosaic virus. *Virology* **204,** 478–481.

Satyanarayana, T., Gowda, S., Boyko, V. P., Albiach-Martí, M. R., Mawassi, M., Navas-Castillo, J., Karasev, A. V., Dolja, V., Hilf, M. E., Lewandowski, D. J., Moreno, P., Bar-Joseph, M., Garnsey, S. M., and Dawson, W. O. (1999). An engineered closterovirus RNA replicon and analysis of heterologous terminal sequences for replication. *Proc. Natl. Acad. Sci. USA* **96,** 7433–7438.

Satyanarayana, T., Gowda, S., Mawassi, M., Albiach-Martí, M. R., Ayllón, M. A., Robertson, C., Garnsey, S. M., and Dawson, W. O. (2000). Closterovirus encoded HSP70 homolog and p61 in addition to both coat proteins function in efficient virion assembly. *Virology* **278,** 253–265.

Satyanarayana, T., Bar-Joseph, M., Mawassi, M., Albiach-Martí, M. R., Ayllón, M. A., Gowda, S., Hilf, M. E., Moreno, P., Garnsey, S. M., and Dawson, W. O. (2001). Amplification of citrus tristeza virus from a cDNA clone and infection of citrus trees. *Virology* **280,** 87–96.

Satyanarayana, T., Gowda, S., Ayllón, M. A., Albiach-Martí, M. R., Rabindran, S., and Dawson, W. O. (2002). The p23 protein of citrus tristeza virus controls asymmetrical RNA accumulation. *J. Virol.* **76,** 473–483.

Shivprasad, S., Pogue, G. P., Lewandowski, D. J., Hidalgo, J., Donson, J., Grill, L. K., and Dawson, W. O. (1999). Heterologous sequences greatly affect foreign gene expression in tobacco mosaic virus-based vectors. *Virology* **255,** 312–323.

Singh, R. N., and Dreher, T. W. (1998). Specific site selection in RNA resulting from a combination of nonspecific secondary structure and -CCR-boxes: Initiation of minus strand synthesis by turnip yellow mosaic virus RNA-dependent RNA polymerase. *RNA* **4,** 1083–1095.

Sivakumaran, K., Chul-Hyun, K., Tayon, R., Jr., and Kao, C. C. (1999). RNA sequence and secondary structural determinants in a minimal viral promoter that directs replicase recognition and initiation of genomic plus-strand synthesis. *J. Mol. Biol.* **294,** 667–682.

Song, C., and Simon, A. E. (1995). Requirement of a 3′-terminal stem-loop in *in vitro* transcription by an RNA-dependent RNA polymerase. *J. Mol. Biol.* **254,** 6–14.

Thompson, J. D., Higgins, D. G., and Gibson, T. J. (1994). CLUSTAL W: Improving the sensitivity of progressive multiple sequence alignment through sequence weighting, position-specific gap penalties and weight matrix choice. *Nucleic Acids Res.* **22,** 4673–4680.

Tretheway, D. M., Yoshinari, S., and Dreher, T. W. (2001). Autonomous role of 3′-terminal CCCA in directing transcription of RNAs by Qβ replicase. *J. Virol.* **75,** 11373–11383.

Turner, R. L., and Buck, K. W. (1999). Mutational analysis of *cis*-acting sequences in the 3′- and 5′-untranslated regions of RNA2 of red clover necrotic mosaic virus. *Virology* **253,** 115–124.

van Rossum, C. M. A., Brederode, F. Th., Neeleman, L., and Bol, J. F. (1997). Functional equivalence of common and unique sequences in the 3′ untranslated regions of alfalfa mosaic virus RNAs 1, 2, and 3. *J. Virol.* **71,** 3811–3816.

Yoshinari, S., and Dreher, T. W. (2000). Internal and 3′ RNA initiation by Qβ replicase directed by CCA boxes. *Virology* **271,** 363–370.

Yoshinari, S., Nagy, P. D., Simon, A. E., and Dreher, T. W. (2000). CCA initiation boxes without unique promoter elements support *in vitro* transcription by three viral RNA-dependent RNA polymerase. *RNA* **6,** 698–707.

Zuker, M., Mathews, D. H., and Turner, D. H. (1999). Algorithms and thermodynamics for RNA secondary structure prediction: A practical guide. *In* "RNA Biochemistry and Bio/Technology" (J. Barciszewski, and B. F. C. Clark, Eds.), pp. 11–43. Kluwer Academic Publishers, Dordrecht/Norwell, MA.